LBL-29825
Preprint

Lawrence Berkeley Laboratory
UNIVERSITY OF CALIFORNIA

Materials & Chemical Sciences Division

Submitted to Physical Review B

Heat Capacity of High Purity $YBa_2Cu_3O_7$ from 0.4 K to 400 K in Applied Magnetic Fields of Zero and 70 kG

W.C. Lee, K. Sun, L.L. Miller, D.C. Johnston, C.A. Swenson, R.A. Klemm, S. Kim, R.A. Fisher, and N.E. Phillips

October 1990

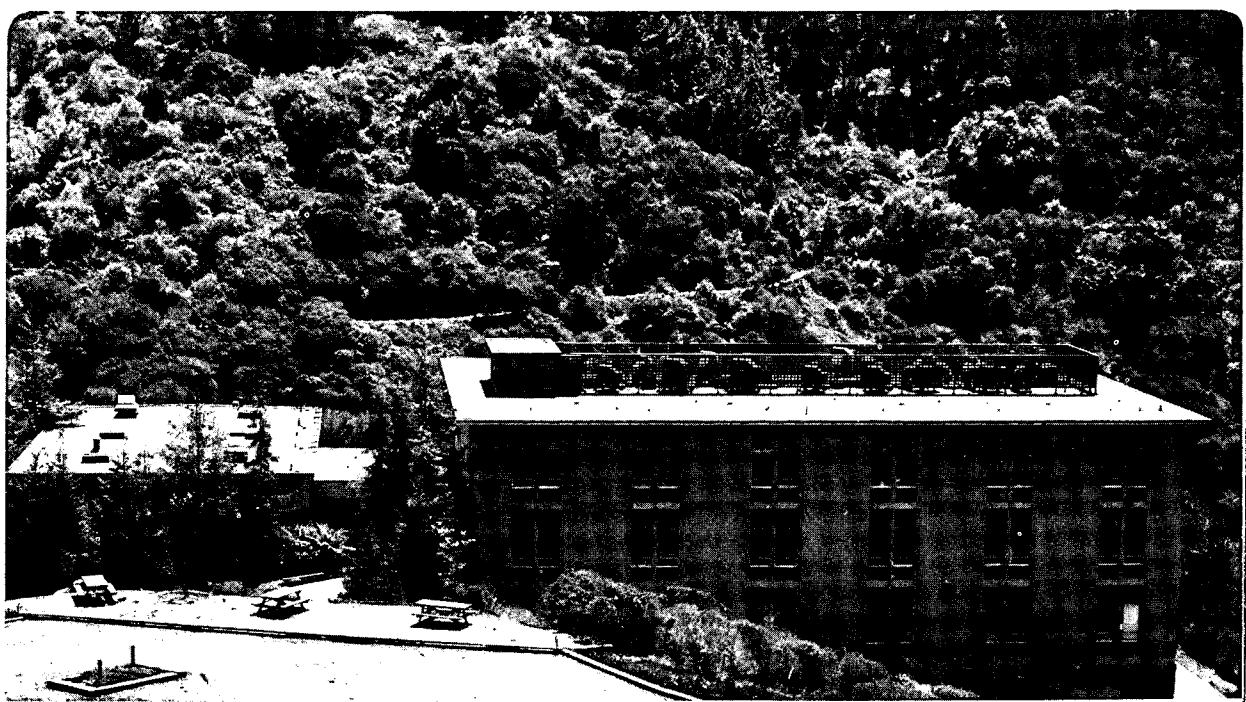

Prepared for the U.S. Department of Energy under Contract Number DE-AC03-76SF00098

DISCLAIMER

HEAT CAPACITY OF HIGH PURITY $YBa_2Cu_3O_7$ FROM 0.4K TO 400 K IN APPLIED MAGNETIC FIELDS OF ZERO AND 70kG

W. C. Lee, K. Sun, L. L. Miller, D. C. Johnston, C. A. Swenson and R. A. Klemm

Ames Laboratory-USDOE and Department of Physics
Iowa State University
Ames, Iowa 50011

S. Kim, R. A. Fisher and N. E. Phillips

Materials and Chemical Sciences Division
Lawrence Berkeley Laboratory
University of California
Berkeley, CA 94720

October 1990

To be published in Phys. Rev. B

The work at Berkeley was supported by the Director, Office of Basic Energy Sciences, Materials Sciences Division of the U.S. Department of Energy under Contract DE-AC03-76SF00098.

Heat Capacity of High Purity $YBa_2Cu_3O_7$ from 0.4 K to 400 K in Applied Magnetic Fields of Zero and 70 kG

W. C. Lee, K. Sun, L. L. Miller, D. C. Johnston,
C. A. Swenson and R. A. Klemm*

Ames Laboratory-USDOE and Department of Physics
Iowa State University, Ames, Iowa 50011

and

S. Kim, R. A. Fisher and N. E. Phillips

Materials and Chemical Sciences Division, Lawrence Berkeley Laboratory
University of California, Berkeley, California 94720

March 6, 1990

1988 PACS Nos. 64.70.Kb, 74.30.Ek, 74.40.+k, 74.70.Vy

Abstract

The heat capacities C(T) of high purity polycrystalline pellet and powder samples of $YBa_2Cu_3O_7$ are reported for the temperature T range 0.4 K to 400 K. In addition to the feature associated with the onset of superconductivity at $T_c \approx 91$ K, two clear anomalies in C(T) for the pellet sample were observed near 74 K and 330 K; the origins of the latter two anomalies is unknown, but the temperatures at which they occur are similar to those at which anomalies are seen in the temperature-dependent magnetization M(T). The anomaly in C(T) at $\approx$ 330 K observed for the pellet was not observed for the powder sample, consistent with lack of an anomaly in M(T) near this temperature for the powder sample. For the pellet sample, the electronic entropy near T_c, the contribution of superconducting fluctuations to C(T) near T_c, and the influence of a 70 kG magnetic field on C(T) near T_c and below 10 K are analyzed and discussed. Various features of the C(T) for the pellet sample such as the magnitude of C(T) and the derived Debye temperature and heat capacity jump at T_c, as well as the size and shape of the C(T) anomalies at $\approx$ 74 K and 330 K, were found to depend on the thermal and/or magnetic field treatment history of the sample. Differential thermal analysis measurements quantitatively determined the $BaCuO_2$ impurity content in our batch of $YBa_2Cu_3O_7$ to be 0.3(1) wt.%. Coupled with analysis of the low T C(T) measurements, we conclude that the intrinsic Sommerfeld coefficient $\gamma(0)$ associated with the $YBa_2Cu_3O_7$ phase in our pellet sample is $\approx$ 4.0 mJ/mole-K^2. It is suggested that some fraction of $\gamma(0)$ could arise from thermal excitation of antiferromagnetic spin waves in the Cu-O chains of the structure.

I. Introduction

Thermodynamic measurements of the high T_c cuprate superconductors can yield important information about the normal and superconducting states. The most well-studied of these materials is the compound $YBa_2Cu_3O_7$.[1,2] Measurements of the temperature T dependent anisotropic magnetic susceptibility $\chi(T)$ of high purity $YBa_2Cu_3O_7$ have revealed that the intrinsic $\chi(T)$ increases monotonically with T from the superconducting transition temperature $T_c \sim 91$ K up to at least 400 K, with negative curvature below ~ 200 K, for applied magnetic fields H both parallel and perpendicular to the CuO_2 planes of the structure.[3,4] This negative curvature was quantitatively modeled as arising from a combination of superconducting fluctuation diamagnetism and a temperature-dependent normal state $\chi(T)$. From the analysis, microscopic parameters associated with the superconducting state were obtained.

From the above $\chi(T)$ data, the magnetic phase impurity and Cu^{+2} magnetic defect levels in the samples from the batch of $YBa_2Cu_3O_7$ measured appeared to be the lowest of any single crystal or polycrystalline sample for which $\chi(T)$ data had been reported. We concluded that it would be worthwhile to carry out extensive heat capacity C(T) measurements on this batch, despite the large number of C(T) studies already reported for this compound.[5] Our primary goals were to (i) determine whether the nonzero Sommerfeld coefficients $\gamma(T = 0) \gtrsim 4$ mJ/mole-K^2 observed in previous low T C(T) studies[6] are comparable to or greater than that for our batch and determine whether our observed $\gamma(T = 0)$ is intrinsic[6] or extrinsic[7], (ii) document the

influence of superconducting fluctuations on C(T) near T_c[8-11] and (iii) ascertain whether the anomalies sometimes observed in $\chi(T)$ measurements near 240 K[12,13] and/or 320 K[12], and in other types of measurements at various temperatures, are also manifested in C(T). Herein, we report extensive measurements of C(T) for the above high purity batch of $YBa_2Cu_3O_7$ which were carried out in an attempt to address these issues.

II. Experimental Details

A 15 g master batch of polycrystalline $YBa_2Cu_3O_{7-\delta}$ was prepared from pre-dried Ames Lab Y_2O_3, 99.999% CuO and 99.9% $BaCO_3$. The stoichiometric mixture of starting materials was ground thoroughly in air using an agate mortar and pestle and fired at 940 °C for 1 day in air in an alumina crucible. Twelve g was then pressed into a 1/2 in. dia. pellet and the remaining 3 g was maintained separately as powder. Both pellet and powder samples were fired at 940 °C for 90 days in air with ten intermediate grindings, followed by heating in O_2 at 640 °C for one day and oven-cooling to room temperature. The final pellet sample had a density of 75% of the theoretical value. From powder x-ray diffraction analysis, the batch of $YBa_2Cu_3O_{7-\delta}$ was single phase with lattice parameters a = 3.712(2) Å, b = 3.895(4) Å and c = 11.685(4) Å, with c/a = 3.061 and $(b - a)/(b + a) = 9.98 \times 10^{-3}$. These values indicate an oxygen deficiency $\delta \sim 0$.[14] The powder sample was examined with an optical microscope and the grains appeared to be well-formed single crystals with a roughly cubic shape with dimensions ~ 25 $(\mu m)^3$;

this was the sample used in our study of the superconducting fluctuation diamagnetism above T_c in $YBa_2Cu_3O_7$.[3]

The results of a differential thermal analysis (DTA) measurement on the powder sample in oxygen gas using a Perkin-Elmer 1700 DTA with a System 7/4 controller are shown in Fig. 1(a). The small endothermic peak with an onset near 925 °C is the melting transition of the Ba- and Cu-rich Y-Ba-Cu-O eutectic composition impurity.[15] In order to ascertain the amount of eutectic impurity present in the $YBa_2Cu_3O_7$ powder, a small powder sample consisting of 90 wt.% powder $YBa_2Cu_3O_7$ was mixed with 5 wt.% $BaCuO_2$ and 5 wt.% CuO and the mixture heated to 960 °C in a tube furnace under O_2 gas to form a eutectic mixture plus $YBa_2Cu_3O_7$ majority phase. A DTA scan as in Fig. 1(a) was then performed, and the results are shown in Fig. 1(b). The ratio of the enthalpy under the peak in Fig. 1(a) to that in Fig. 1(b) indicates that (0.6 ± 0.2) wt.% of our $YBa_2Cu_3O_7$ powder sample consists of the eutectic impurity mixture. Since this consists of little Y_2O_3 and approximately equal amounts of CuO and $BaCuO_2$,[15] our batch contains 0.3(1) wt.% $BaCuO_2$.

Heat capacity C(T) measurements from 0.4 K to 110 K were carried out on the pellet sample of $YBa_2Cu_3O_7$ using pulse calorimeters at Ames (1.5 K to 105 K, accuracy of 1-2%) and at Berkeley (0.4 K to 30 K). The Berkeley measurements were performed in either zero applied magnetic field or in a field H = 70 kG in order to to estimate the concentration of (nearly) magnetically isolated Cu^{+2} local magnetic moments in the sample, and thereby deduce information about the intrinsic low temperature Sommerfeld heat capacity coefficient $\gamma(0)$.

C(T) data for both the powder and pellet samples were obtained between 110 K and 400 K using a Perkin Elmer 7700 Differential Scanning Calorimeter (DSC) at a T ramp rate of 10 °C/min in a search for possible phase transitions. For comparison with these C(T) data, magnetic susceptibility $\chi(T)$ data for the same samples were obtained at Ames using a Quantum Design SQUID magnetometer.

In the Ames pulse C(T) measurements, which were carried out first, we used a small amount of Apiezon N grease to attach the sample to a copper plate, with the thermometer attached to the opposite side of the plate. For the pulse C(T) measurements at Berkeley, the sample was wrapped with silver foil to enhance the thermal contact between sample and addenda and attached to a copper plate with a small amount of GE 7031 varnish. A small thin-film heater was mounted onto the silver foil. In these measurements, the duration of a heat pulse was about 2 min at high temperatures and 30 s below 30 K. The thermal equilibration time was about 5 and 10 min in the respective T ranges.

Additional C(T) measurements, accurate to 0.5%, were made on the pellet sample in Berkeley in $H = 0$ and $H = 70$ kG from 68 K to 110 K using a high resolution continuous heating method and the same sample mounting and addenda as for the pulsed measurements, with a heating rate of $\simeq 4$ mK/s. A series of four measurements were made, with one in the 70 kG field. Three zero-field measurements were made to determine the reproducibility of the measurements and the possible influence of the thermal and magnetic field history of the sample on its heat capacity.

III. Results

An overview of C(T) of our $YBa_2Cu_3O_7$ pellet sample in zero applied magnetic field from 1.5 K to 400 K is shown in Fig. 2(a) (C vs. T) and Fig. 2(b) (C/T vs. T). There is good agreement between the C(T) near 110 K measured using the pulsed and continuous heating calorimeters and that measured using the DSC. The magnitude of the heat capacity over the whole temperature range is similar to the results of previous measurements on relatively magnetically pure samples.[5,16,17]

To ascertain the reproducibility of the heat capacity near T_c, a series of four measurements was carried out using the Berkeley continuous heating calorimeter. Initially, the sample was cooled from room temperature to 65 K and held at that temperature overnight. Curve A in Fig. 3 shows the first measurement (H = 0) up to ≈ 110 K. A feature with a peak near 89.5 K is clearly observed, associated with the onset of superconductivity. The sample was then cooled again to 65 K, held overnight, and the measurement repeated (labeled B in Fig. 3). The peak in C/T for B increased to 91.0 K from the value of 89.5 K found for A. From Fig. 3, large differences between the two measurements are seen in both the magnitude of C(T) and the size of the feature near T_c. Also, there are hints of anomalies near 102 K and 75 K in B not evident in A. There were no differences apparent to us in the manner in which the data sets A and B were accumulated and analyzed.

Next, the sample was again cooled to 65 K and held overnight. A magnetic field of 70 kG was applied, and C(T) measured (curve C in Fig. 3) in the same manner as in the first two experiments. The feature at T_c is smeared out by the field as reported earlier,[5,18] and the

temperature of the maximum in C/T has decreased to 88.5 K. There is a clear crossover of the data sets B and C near 85 K. Below 65 K and above 95 K, the B and C data sets coincide, and both show evidence of a feature at 102 K. After measurement C, the sample was warmed to room temperature, cooled to 65 K in zero field and held overnight, and a fourth data set obtained (set D in Fig. 3) using the same heating rate as before. Remarkably, the weak anomaly at 75 K in set B appears now as a sharp mean-field-like second order transition in set D.

The results of the pulse C(T) measurements in zero field from 0.5 K to 10 K at Ames and at Berkeley are shown in Fig. 4. Fig. 5 shows the data obtained at Berkeley in both zero field and 70 kG. The zero field heat capacity measurements show a clear upturn in C/T below about 2 K. In H = 70 kG, a clear Schottky-like anomaly appears with a peak near 3 K; at very low T (< 0.5 K), a sharp upturn in C/T is observed.

An expanded plot of the DSC data for the pellet sample of $YBa_2Cu_3O_7$ in Fig. 2(a) from 120 K to 400 K taken with increasing T is shown in Fig. 6, where data for the same sample with decreasing T and for the powder sample with increasing T are also included. With increasing T, an anomaly near 330 K is seen for the pellet sample which is not obviously present in the measurement with decreasing T. From Fig. 6, there is no evidence of an anomaly near 220 - 240 K. There is also no evidence of any anomalies in C(T) for the powder sample upon increasing or decreasing (not shown) the temperature.

Magnetic susceptibility $\chi(T)$ data above T_c for the pellet and powder samples of $YBa_2Cu_3O_7$ in fields of 30 or 50 kG are shown in Fig. 7. The powder was aligned with the c-axis parallel to the field

using a method described previously,[3] whereas the grains in the pellet were found using x-ray diffraction of the surface to be randomly aligned. The data for the pellet sample show a clear cusp at ≈ 320 K whereas the data for the powder exhibit no evidence of an anomaly above T_c. Because of the proximity of the cusp temperature for the pellet to that of the heat capacity anomaly observed above with the DSC on heating, the source of the anomalies in the two types of measurement may be the same.

Magnetization vs. temperature data below T_c for the pellet sample in fields of 50 G and 50 kG are shown in Fig. 8. The low-field data show a sharp superconducting onset at 91.8 K, and a shielding fraction of 127% uncorrected for demagnetization factors. The 50 kG data exhibit an anomaly near 75 K. This anomaly might be a manifestation of flux-pinning effects, although this appears unlikely because the magnetization is reversible with increasing and decreasing field at this field and temperature.[19] Alternatively, it could be a reflection of some sort of phase transition occurring at this temperature as is suggested clearly in the C(T) data set D for the pellet in Fig. 3.

IV. Analysis and Discussion

A. Heat Capacity near T_c

Here we will discuss the results in Fig. 3 of the set of four sequential C(T) measurements using the continuous heating method at Berkeley. The differences between the first data set A in zero field and the subsequent zero field sets B and D are striking. Near T_c, the heat capacity in B is about 6% less than in A. Using the traditional method of entropy balance to estimate the heat capacity jump at T_c (but see below), one obtains $\Delta C/T_c$ = 32 mJ/K^2-mole $YBa_2Cu_3O_7$ for B, which is 42% less than the value of 55 mJ/mole-K^2 for A. These differences may be compared with the absolute accuracy of each measurement of 0.5% and with an expected reproducibility much better than this. Thus, these differences are real and must arise from a thermal history dependence of the heat capacity. Smaller differences are apparent between the data sets B and D. In D, a sharp anomaly at about 74 K is observed which appears to be smeared out in set B and absent in set A; this anomaly occurs at about the same temperature as that seen in the magnetization data at 50 kG in Fig. 8.

In an applied field of 70 kG, the heat capacity in a plot of C/T vs. T (data set C) shows a smooth, broad peak at T_c and only a slight downward shift in the peak temperature compared with the zero field data, as previously reported.[5,18] As noted above, a sharp anomaly was observed at 74 K in data set D; these data were taken in zero field after the high field set C was obtained. Thus, although it seems unlikely, the magnetic field history of the sample may be involved with the apparent irreproducibility of C(T) in Fig. 3, in addition to the

above influence of the thermal history. The C/T data set C in H = 70 kG is larger in magnitude than the zero field set B between ≈ 75 K and ≈ 85 K, whereas it is smaller between ≈ 85 K and ≈ 93 K. In the latter region, the entropy change $\Delta S = S(0) - S(70\ kG) \approx 83$ mJ/mole-K, and in the former it is -55 mJ/mole-K, yielding a net entropy change $\Delta S_{net} = 28$ mJ/mole-K. This apparent non-conservation of entropy could conceivably arise through the above thermal history dependence of C(T) and/or from the limited temperature range of the measurements in Fig. 3.

Due to lack of detailed knowledge of the dominant lattice contribution to the heat capacity of high T_c cuprate superconductors near T_c, it is not clear how to accurately separate the observed heat capacity into electronic and lattice parts. A further complication is that close to T_c, the thermodynamic and electronic transport properties of the cuprate superconductors are dominated by the influence of superconducting fluctuations.[4] Therefore, without taking into account the fluctuation term, one might infer an inaccurate mean-field heat capacity jump ΔC at T_c, which would then lead to an inaccurate estimate of the normal state Summerfeld coefficient γ if one used, e.g., the BCS result relating γ to ΔC ($\Delta C/\gamma T_c = 1.43$).

We now consider the fluctuation contribution to the observed C(T) to lowest order. After Refs. 3 and 4, we utilize a model in which there are two conducting layers per unit cell in $YBa_2Cu_3O_7$, each of which is assigned one complex s-wave order parameter; the layers are coupled by Josephson tunneling. Above T_c, the relationship between the superconducting fluctuation heat capacity $C_{fl}^{\ddagger}(T)$ and the superconducting fluctuation diamagnetism $\chi_c^{fl}(T)$ with H || c is given by[4]

$$C^{+}_{fl}(T) = - \frac{3\phi_o^2 \chi_c^{fl}(T)}{4\pi^2 T \xi_{ab}^4(0)} \propto -\chi_c^{fl}(T)/T , \qquad (1)$$

where ϕ_o is the flux quantum hc/2e and $\xi_{ab}(0)$ is the zero-temperature Ginzburg-Landau coherence length within a CuO_2 layer. Below T_c in the three-dimensional fluctuation region, the fluctuation heat capacity $C^{-}_{fl}(T)$ is reduced from $C^{+}_{fl}(T)$ by $\sim 1/\sqrt{2}$.[4,8,20]

Using Eq. (1), the measured $\chi_c^{fl}(T)$ and the derived $\xi_{ab}(0)$, one can estimate the contributions $C^{+}_{fl}(T)$ and $C^{-}_{fl}(T)$ to the measured C(T) above and below T_c, respectively. Then, by subtracting these contributions from C(T), an estimate of the sum of the lattice and electronic heat capacities in the absence of superconducting fluctuations (mean-field heat capacity C_{MF}) can be obtained. Here, we do not account for the superconducting transition width[4,21] arising from chemical inhomogeneity in the sample. Therefore, the calculated fluctuation heat capacity diverges close to T_c (Fig. 9), in contrast to our observations. For temperatures somewhat removed from the average T_c, we expect the calculated fluctuation contributions to more accurately apply to the observations.

In Fig. 10(a), we replot the observed C/T vs. T data set D in Fig. 3 (crosses) and $C_{MF}(T)$ derived as described above (open circles) for the temperature ranges 81 - 85 K and 95 to 101 K, using $\xi_{ab}(0)$ = 13.6 Å and $\chi_c^{fl}(T)$ from Ref. 3. For the temperature region closer to T_c, we linearly extrapolated $C_{MF}(T)$ on both sides of T_c to T_c (solid lines). T_c was taken to be 90.8 K, the temperature at which a pulsed C(T) data set taken at Ames over a limited temperature range spanning T_c (not

presented here) showed a sharp cusp. This is also the temperature at which the magnetization data for H = 50 G in Fig. 8 showed a sharp onset, and is the average peak temperature of C(T)/T for data sets A, B and D in Fig. 3. From Fig. 10(a), the mean-field heat capacity jump at T_c is inferred to be $\Delta C_{MF}(T_c)/T_c \simeq 33$ mJ/mole-K^2, coincidentally nearly the same as the above value $\Delta C/T_c = 32$ mJ/mole-K^2 obtained using conventional entropy balance near T_c. The value of ΔC_{MF} yields $\gamma_{MF} \simeq 23$ mJ/mole-K^2 using the above BCS weak coupling mean-field result. This γ_{MF} value is less than most reported γ values.[5,6,17] However, this value is consistent with the value (26 mJ/mole-K^2) obtained from a free electron gas analysis of the spin susceptibility[3] above T_c derived from $\chi(T)$ data as in Fig. 7. We estimate the density of states at the Fermi energy to be $D(E_F) = 3.3$ states/eV-Cu atom using the relation $\gamma_{MF} = \pi^2 \mu_B^2 D(E_F)/3k_B$.

A similar analysis of the C(T) data set A in Fig. 3 is shown in Fig. 10(b). Here, we find $\Delta C_{MF}/T_c = 64$ mJ/mole-K^2, and $\gamma_{MF} = 44$ mJ/mole-K^2 in the BCS weak coupling limit. The $\Delta C_{MF}/T_c$ value is somewhat larger than the above value $\Delta C/T_c = 55$ mJ/mole-K^2 obtained using conventional entropy balance near T_c.

B. Heat Capacity between 0.4 K and 10 K

The Ames and Berkeley pulse calorimeter measurements are in agreement below ~ 5 K, as seen in Fig. 4. At higher temperatures, a large difference becomes apparent; both measurements are accurate to 1-2% below 30 K, so this difference is real. The source of this difference between the two C(T) data sets above 5 K is not known. This

difference amounts to a difference in the lattice heat capacity apparently induced by changes in the thermal and/or magnetic field history of the sample, as documented near T_c in Fig. 3 and above 120 K in Fig. 6. The two C(T) data sets in Fig. 4 yield Debye temperatures differing by more than 30 K (see below).

In Figs. 4 and 5, the low-temperature upturn in C(T, H = 0)/T starts near 2 K, arising primarily from magnetically isolated Cu^{+2} local magnetic moments. A common impurity in $YBa_2Cu_3O_7$ samples is $BaCuO_2$,[22,23] and is one of the components of the eutectic impurity present in our samples as documented above. Some samples of $BaCuO_2$ exhibit C(T)/T behavior nearly independent of T at low T, while others show an upturn.[22,24] Considering the presence of this impurity phase as well as localized Cu^{+2} moments in our samples of $YBa_2Cu_3O_7$, we fit our zero-field C(T) data with the expression

$$C(T) = \frac{A_{-2}}{T^2} + \gamma^*(0)T + B_3T^3 + B_5T^5 + B_7T^7 \quad , \qquad (2)$$

where the first term accounts for the low T upturn, the second is a linear term of unknown origin, and the remaining terms are due to the lattice contribution. Fitting Eq. (2) to the zero-field data in Fig. 5 yields A_{-2} = 13.1(3) mJ-K/mole, $\gamma^*(0)$ = 5.0(1) mJ/mole-K^2, B_3 = 0.33(1) mJ/mole-K^4, B_5 = 4.22(8) x 10^{-3} mJ/mole-K^6, and B_7 = 2.02(4) x 10^{-5} mJ/mole-K^8. From the value of B_3, the calculated Debye temperature Θ_D = 422(8) K, which is similar to reported values.[5,25,26] For the Ames C(T) data set in Fig. 4, $\gamma^*(T = 0)$ = 5.7(6) mJ/mole-K^2, which is equal within experimental error with the value from the Berkeley data, whereas

Θ_D = 456 K, about 30 K larger than the Berkeley value. The large difference between the Ames and Berkeley data sets between 5 K and 10 K is real, as noted above, and apparently arises from the different thermal histories of the sample in the two measurements.

It is known that a sufficiently high magnetic field can cause the C(T)/T upturn for H = 0 to become a Schottky-like anomaly.[27] In Fig. 5 for H = 70 kG, there is indeed a broad maximum in C(T)/T near 3 K and there is a sharp upturn at much lower temperature. This sharp upturn is from the coupling between the magnetic field and the Cu nuclear moments.[27,28] To analyze the H = 70 kG results, we used the expression

$$C(T) = \frac{A_{hf}}{T^2} + n_i C_{Sch}(T) + \gamma^*(H)T + C_{lattice} \quad , \qquad (3a)$$

with

$$C_{Sch}(T) = R \frac{\delta^2}{T^2} \frac{e^{\delta/T}}{(1 + e^{\delta/T})^2} \quad , \qquad (3b)$$

where the first term in Eq. (3a) is due to the hyperfine interaction, the next term is the Schottky anomaly due to n_i mole fraction of isolated Cu^{+2} defects, $C_{Sch}(T)$ is the heat capacity per mole of these defects, and $\gamma^*(H)T$ is the linear contribution in the 70 kG magnetic field. In Eq. (3b), R is the molar gas constant and δ is the energy splitting in K of the spin 1/2 Zeeman levels in the field H: $\delta = \mu_B H/k_B$, assuming a gyromagnetic factor g = 2. From a fit to the data on a CT^2 versus T^3 plot at low T, we find A_{hf} = 0.47(1) mJ-K/mole $YBa_2Cu_3O_7$, which is close to the theoretical value of 0.50 mJ-K/mole for

the three moles of Cu, two of Ba and one of Y nuclei in one mole of $YBa_2Cu_3O_7$.[5,10,28] $\gamma^*(H = 70\ kG)$ is found to be 6.5(2) mJ/mole-K^2. From $\gamma^*(H = 0)$ and $\gamma^*(H = 70\ kG)$, we have $\partial\gamma^*/\partial H \simeq 0.021$ mJ/mole-K^2-kG, which is similar to the reported value.[10] By subtracting the hyperfine, linear and lattice (from the H = 0 fit) terms from the observed C(T, H = 70 kG) data according to Eq. (3a), the experimental isolated Cu^{+2} contribution to C(T, H = 70 kG) was computed and is plotted vs. T in Fig. 11 (open circles). Also shown is the theoretical Schottky contribution $n_i C_{Sch}(T)$ from Eq. (3b) for $n_i = 0.0044$ (solid curve).

The impurity mole fraction due to isolated Cu^{+2} defects, n_i, was found above to be 0.0044(1) mole Cu^{+2}/mole $YBa_2Cu_3O_7$. This could arise from isolated defects in the $YBa_2Cu_3O_7$ majority phase lattice itself and/or in the $BaCuO_2$ impurity lattice. The latter possibility is supported by the magnetic field dependence of C(T) for $BaCuO_{2+x}$.[29] The above DTA measurements revealed the presence of 0.3(1) wt.% $BaCuO_2$ impurity phase in our batch of $YBa_2Cu_3O_7$ sample. If the upturn in the zero field C(T) and the Schottky-like anomaly in C(T, H = 70 kG) are generated from all of the Cu^{+2} moments in this amount of $BaCuO_2$, one would expect $n_i = 0.014(5)$ mole Cu^{+2}/mole $YBa_2Cu_3O_7$, significantly greater than the observed n_i value. Thus, the bulk of the Cu^{+2} ions in the $BaCuO_2$ impurity phase do not contribute to the zero-field low-temperature upturn in the observed C(T).

Our non-zero $\gamma^*(T = 0, H = 0) \equiv \gamma^*(0)$ value evidently arises from the $YBa_2Cu_3O_7$ phase and/or the bulk $BaCuO_2$ (BCO) impurity phase (the contribution to $\gamma^*(0)$ from CuO impurity is negligible). We consider

first the second possibility. The above value of 0.3(1) wt.% $BaCuO_2$ corresponds to n_{BCO} = 0.014(5) moles $BaCuO_2$/mole $YBa_2Cu_3O_7$. For $BaCuO_2$ heat-treated in a way similar to the preparation of our samples of $YBa_2Cu_3O_7$, one expects $\gamma_{BCO} < 80$ mJ/mole $BaCuO_2$ from published heat capacity data.[22] Thus, we expect the impurity contribution γ_i to our measured $\gamma^*(0)$ for $YBa_2Cu_3O_7$ to be given by $\gamma_i = n_{BCO}\gamma_{BCO} < 0.7(2)$ mJ/K^2-mole $YBa_2Cu_3O_7$. This value is much less than the above observed values $\gamma^*(0)$ = 5.0(1) and 5.7(6) mJ/mole-K^2. We conclude that the intrinsic $\gamma(0)$ associated with the $YBa_2Cu_3O_7$ phase in our pellet sample is $\gamma(0) \approx 4.0$ mJ/mole-K^2. A similar value was obtained by Reeves et al.,[30] based on a Raman scattering determination of the $BaCuO_2$ concentration, coupled with low temperature C(T) measurements.

The question now arises as to whether this $\gamma(0)$ is intrinsic to a perfectly ordered $YBa_2Cu_3O_7$ lattice, or whether it arises in some way from the presence of lattice disorder. One scenario presented recently is that lattice disorder and the presence of resultant localized Cu^{+2} magnetic moments produces normal (non-superconducting) regions in the sample, resulting in a non-zero $\gamma(0)$ and an upturn in the zero-field C(T)/T associated with those regions.[7]

An alternative explanation which could give rise to an intrisic $\gamma(0) > 0$ for $YBa_2Cu_3O_7$ is as follows. The Cu ions in the CuO_2 planes and Cu-O chains of the structure appear to be essentially localized Cu^{+2} ions with spin 1/2.[31,32] Elementary spin wave theory predicts that spin waves on a one-dimensional chain of spins 1/2, with nearest neighbors antiferromagnetically coupled with exchange energy $E_{ij} = JS_i \cdot S_j$, should exhibit a magnetic molar heat capacity C_M which is linear

in temperature and given by $C_M = (\pi/3\sqrt{2})R\cdot(T/J) = (1231\ mJ/mole\text{-}K)(T/J)$, where J is in units of K. If one assumes that spin waves propagate along the Cu-O chains (where the Cu ions are assumed to be spin 1/2 Cu^{+2} ions) of $YBa_2Cu_3O_7$, which contains one chain Cu atom/formula unit, then an intrinsic linear term would be expected in the C(T), with a magnitude of the observed order. For example, the above $\gamma(0) \approx 4\ mJ/mole\text{-}K^2$ predicts that $J \approx 300$ K, comparable in magnitude with the value (~ 1500 K) inferred[32] for the coupling strength between Cu ions within the CuO_2 planes of the structure. This hypothesis would explain the lack[5] of a linear term in the low temperature C(T) for the Bi- and Tl-based cuprate superconductors, since these structures do not contain Cu-O chains. The existence of the spin waves in the Cu-O chains of $YBa_2Cu_3O_7$ necessary to this hypothesis can be tested via inelastic neutron scattering experiments on large single crystals of $YBa_2Cu_3O_7$.

C. Heat Capacity above 120 K

Our $\chi(T)$ data for the pellet sample in Fig. 6 partially confirm previous $\chi(T)$ measurements[12,13] that anomalies sometimes occur at ~ 240 K, ~ 330 K, or both. The data for this sample show only the anomaly near 330-350 K with no obvious anomaly near 240 K. Our C(T) data for the pellet sample taken on warming show an anomaly at ~ 330 - 350 K, and therefore appear to confirm that the corresponding anomaly in $\chi(T)$ is a bulk effect and not due to impurity phases. However, the anomaly in the C(T) data for the pellet sample was not unambiguously observed on cooling, possibly due to the above thermal history dependence of C(T). $\chi(T)$ and C(T) data for our powder sample

taken on warming from 120 K to 400 K and cooling from 400 K to 120 K showed no anomalies.

V. Concluding Remarks

We have accomplished some of the goals of our heat capacity C(T) study of high purity $YBa_2Cu_3O_2$ enumerated in Sect. I. From a determination of the $BaCuO_2$ magnetic impurity phase concentration in our batch of this compound from differential thermal analysis measurements, coupled with analysis of low (> 0.4 K) temperature C(T) measurements in zero and 70 kG applied magnetic fields, we conclude that the Sommerfeld heat capacity coefficient intrinsic to the $YBa_2Cu_3O_7$ phase in our pellet sample is $\gamma(0) \approx 4.0$ mJ/mole-K^2. The origin of this $\gamma(0)$ is not yet clear. One possibility which is often considered is that this $\gamma(0)$ is an indication that part of the sample does not become superconducting; i.e., $\gamma(0)/\gamma$ is the normal fraction, where γ is the normal state Sommerfeld coefficient.[5,7,33] We suggest that some fraction (unknown as yet) of $\gamma(0)$ could also arise from thermal excitation of spin waves on the Cu-O chains, and could therefore be intrinsic to an atomically ordered $YBa_2Cu_3O_7$ structure. We hope that this hypothesis will be tested using inelastic neutron scattering measurements on large single crystals.

It is clear by now that superconducting fluctuations have a dramatic influence on the thermodynamic and electronic transport properties of the high T_c cuprates in the vicinity of T_c.[3,4,8-11,18,34] Heat capacity measurements on single crystals of $YBa_2Cu_3O_7$ near T_c show strong evidence for a non-mean-field shape,

attributed to these fluctuations.[8,18] However, even slight broadening of the superconducting transition, as in most polycrystalline samples of $YBa_2Cu_3O_7$, rapidly smooths out this shape to appear mean-field-like.[21] Indeed, a mean-field-like shape was found for our pellet sample. Utilizing the data and theory in Refs. 3 and 4, a quantitative estimate of the fluctuation heat capacity was made and found to be significant on the scale of the measurements in Fig. 3. A lowest-order attempt was made to extract the mean-field heat capacity in the absence of the fluctuations. We find that the heat capacity jump at T_c, deduced from C(T) data using the conventional entropy balance technique, may be appreciably affected by the presence of the fluctuations.

There have been numerous reports in the literature of anomalies occurring at various temperatures in various measurements of $YBa_2Cu_3O_7$ which have not been confirmed as magnetic or structural transitions by neutron or x-ray scattering techniques.[12,13,26,35] We presented calorimetric evidence that one such anomaly in the magnetic susceptibility $\chi(T)$ at ~ 310-330 K[12] is a bulk phase transition of some kind. The occurrence of these transitions is highly sample-dependent, and it is not known what characteristics of the samples control their occurrence.[12,26] In our experiments, for example, we found that the powder sample of $YBa_2Cu_3O_7$ did not show the anomalies at ~ 330 K in C(T) and $\chi(T)$ seen for the pellet sample.

Finally, and unexpectedly, our C(T) measurements on the pellet sample of $YBa_2Cu_3O_7$ revealed a surprisingly strong influence of the thermal and/or magnetic field history of the sample. The magnitude of C(T) in both the low (5 - 10 K) and higher (70 - 120 K) T regimes were

strongly influenced by the thermal/magnetic field history. The heat capacity jump at T_c and Debye temperature (but not the $\gamma^*(0)$ value) derived from these data were quite different for different experiments, and the shape and size of the 74 K anomaly were also strongly history dependent. These types of effects have been observed in elastic measurements of various types, where it is found that such effects are highly sample dependent.(26) Thus, for example, the heat capacities of some samples of $YBa_2Cu_3O_7$ are highly stable with time and thermal cycling.(33)

Acknowledgments

The Ames group thanks A. Bevolo for use of his optical microscope and R. W. McCallum for extensive discussions of the Y_2O_3-CuO-BaO phase diagram and assistance with the DTA measurements. Ames Laboratory is operated for the U. S. Department of Energy by Iowa State University under contract No. W-7405-Eng-82. The work at Ames was supported by the Director for Energy Research, Office of Basic Energy Sciences. The work at Berkeley was supported by the Director, Office of Energy Research, Office of Basic Energy Sciences, Material Sciences Division of the U. S. Department of Energy under Contract No. DE-AC03-76SF00098.

*Present address: Solid State Division, Oak Ridge National Laboratory, P. O. Box 2008, Oak Ridge, TN 37831-6032

References

1. Proc. Internat. Conf. on High Temperature Superconductors and Materials and Mechanisms of Superconductivity, Interlaken, Switzerland, 28 Feb.-4 Mar., 1988, Physica C 153-155 (1988).

2. Proc. Internat. Conf. on High Temperature Superconductors and Materials and Mechanisms of Superconductivity II, Stanford, CA, 23-28 July, 1989; Physica C 162-164 (1989).

3. W. C. Lee, R. A. Klemm, and D. C. Johnston, Phys. Rev. Lett. 63, 1012 (1989); W. C. Lee and D. C. Johnston, Phys. Rev. B 41, 1904 (1990).

4. R. A. Klemm, Phys. Rev. B 41, 2074 (1990).

5. For a review, see R. A. Fisher, J. E. Gordon and N. E. Phillips, J. Supercond. 1, 231 (1988).

6. For a review, see S. E. Stupp and D. M. Ginsberg, Physica C 158, 299 (1989).

7. Norman E. Phillips, R. A. Fisher, J. E. Gordon and S. Kim, Ref. 2, p. 1651; Norman E. Phillips, R. A. Fisher, J. E. Gordon, S. Kim, A. M. Stacy, M. K. Crawford, and E. M. McCarron III, unpublished.

8. S. E. Inderhees, M. B. Salamon, N. Goldenfeld, J. P. Rice, B. G. Pazol and D. M. Ginsberg, Phys. Rev. Lett. 60, 1178 (1988); (E) ibid. 60, 2445 (1988).

9. T. Laegreid, P. Tuset, O.-M. Nes, M. Slaski, and K. Fossheim, Ref. 2, p. 490.

10. R. A. Fisher, J. E. Gordon, S. Kim, N. E. Phillips and A. M. Stacy, Ref. 1, p. 1092.

11. J. E. Gordon, M. L. Tan, R. A. Fisher, and N. E. Phillips, Solid State Commun. 69, 625 (1989); Ref. 2, p. 484.

12. D. C. Johnston, S. K. Sinha, A. J. Jacobson, and J. M. Newsam, Ref. 1, p. 572; unpublished.

13. M. Miljak, G. Collin and A. Hamzic, J. Magn. Magn. Mater. 76-77, 609 (1988); M. Miljak, G. Collin, A. Hamzic, and V. Zlatic, Europhys. Lett. 9, 723 (1989).

14. D. C. Johnston, A. J. Jacobson, J. M. Newsam, J. T. Lewandowski, D. P. Goshorn, D. Xie and W. B. Yelon, Am. Chem. Soc. Symp. Ser. 351, 136 (1987).

15. R. W. McCallum, J. Metals 41, 50 (1989); private communication.

16. K. Sun, L. L. Miller, and D. C. Johnston, unpublished.

17. A. Junod et al., Physica C 159, 215 (1989).

18. M. B. Salamon, S. E. Inderhees, J. P. Rice, B. G. Pazol, D. M. Ginsberg and N. Goldenfeld, Phys. Rev. B 38, 885 (1988).

19. Sreeparna Mitra, J. H. Cho, W. C. Lee, D. C. Johnston, and V. G. Kogan, Phys. Rev. B 40, 2674 (1989).

20. P. Muzikar, Phys. Rev. Lett. 61, 479 (1988); H. R. Brand and M. M. Doria, ibid. 61, 480 (1988); S. E. Inderhees, M. B. Salamon, N. Goldenfeld, J. P. Rice, B. G. Pazol, D. M. Ginsberg, J. Z. Liu, and G. W. Crabtree, ibid. 61, 481 (1988).

21. F. Sharifi, J. Giapintzakis, D. M. Ginsberg and D. J. Van Harlingen, Physica C 161, 555 (1989).

22. R. Kuentzler, Y. Dossmann, S. Vilminot and S. El Hadigui, Solid State Commun. 65, 1529 (1988).

23. S. Eriksson, L.G. Johansson, L. Börjesson, and M. Kakihana, Ref. 2, p. 59.

24. D. Eckert, A. Jonod, T. Graf, and J. Muller, Ref. 1, p. 1038.

25. S. von Molnar, A. Torressen, D. Kaiser, F. Holtzberg and T. Penny, Phys. Rev. B 37, 3762 (1988).

26. C. A. Swenson, R. W. McCallum, and K. No, Phys. Rev. B 40, 8861 (1989).

27. E. S. R. Gopal, Specific Heats at Low Temperatures (Plenum Press, New York, 1966), p. 102.

28. O. V. Lounasmaa, Phys. Rev. 128, 1136 (1962).

29. R. Ahrens, T. Wolf, H. Wohl, H. Rietschel, H. Schmidt, and F. Steglisch, Ref. 1, p. 1008.

30. M. E. Reeves, S. E. Stupp, T. A. Friedmann, F. Slakey, D. M. Ginsberg, and M. V. Klein, Phys. Rev. B 40, 4573 (1989).

31. M. Horvatic, P. Segransan, C. Berthier, Y. Berthier, P. Butaud, J. Y. Henry, M. Couach, and J. P. Chaminade, Phys. Rev. B 39, 7332 (1989).

32. C. H. Pennington, D. J. Durand, C. P. Slichter, J. P. Rice, E. D. Bukowski, and D. M. Ginsberg, Phys. Rev. B 39, 274 (1989).

33. A. Junod, D. Eckert, T. Graf, G. Triscone, and J. Muller, Ref. 2, p. 842.

34. See references cited in Refs. 3,4,8-11,18.

35. See, e.g., S. Bhattacharya, M. J. Higgins, D. C. Johnston, A. J. Jacobson, J. P. Stokes, J. T. Lewandowski and D. P. Goshorn, Phys. Rev. B 37, 5901 (1988), and references therein.

Figure Captions

Fig. 1 Differential thermal analysis scans in O_2 gas for (a) our $YBa_2Cu_3O_7$ powder sample, and (b) a mixture of 90 wt.% of the powder sample with 5 wt.% CuO and 5 wt.% $BaCuO_2$.

Fig. 2 (a) Overview of heat capacity C vs. temperature T for a polycrystalline $YBa_2Cu_3O_7$ pellet sample in zero applied magnetic field from pulsed calorimeter measurements at Ames (< 110 K), pulsed calorimeter measurements at Berkeley (1 - 30 K), continuous heating calorimeter measurements at Berkeley (68 - 110 K, top data set here, set A in Fig. 3), and differential scanning calorimeter measurements at Ames (110 - 400 K).

(b) C/T vs. T data derived from (a).

Fig. 3 Heat capacity divided by temperature C/T vs. T for $T \sim T_c$ measured at Berkeley using a continuous heating technique for the $YBa_2Cu_3O_7$ pellet sample. The sequence was as follows. A: cooled from room temperature and held overnight at 65 K in zero applied magnetic field H before measurement; B: cooled from 110 K and held at 65 K overnight (H = 0); C: cooled from 110 K and held at 65 K overnight, then H = 70 kG applied; D: cooled from room temperature (H = 0) and held at 65 K overnight.

Fig. 4 Low temperature pulsed heat capacity divided by temperature C/T vs. T^2 in zero field measured at Ames (squares) and Berkeley (circles).

Fig. 5 Low temperature pulsed heat capacity divided by temperature C/T vs. T^2 measured at Berkeley with H = 0 (circles) and 70 kG (crosses); the zero-field data are the same as in Fig. 4 from Berkeley. The solid curve is a fit to the zero-field data (see text).

Fig. 6 Heat capacity C vs. temperature T measured at Ames using a differential scanning calorimeter with a temperature scanning rate of 10 °C/min. The solid data set was taken on heating the $YBa_2Cu_3O_7$ pellet sample, the long-dashed data on cooling the pellet sample, and the short-dashed data on heating the powder sample.

Fig. 7 Magnetic susceptibility χ vs. temperature from 95 K to 400 K for $YBa_2Cu_3O_7$. Open circles: 191 mg piece of the pellet sample with randomly oriented grains (H = 50 kG); crosses: 17.6 mg of the powder sample with the grains aligned with c || H (H = 30 kG).

Fig. 8 Magnetization M vs. temperature for a piece of the pellet sample of $YBa_2Cu_3O_7$ in applied fields of 50 G (filled circles) and 50 kG (open squares).

Fig. 9 Superconducting fluctuation heat capacity divided by temperature C_{fl}/T vs. T, calculated using the data and parameters from Ref. 3.

Fig. 10 (a) Observed heat capacity (plus symbols) from data set D in Fig. 3 compared with the sum of the estimated mean-field electronic and lattice heat capacities (solid lines).
(b) Same as (a), but for data set A from Fig. 3.

Fig. 11 Heat capacity of the magnetically isolated Cu^{+2} magnetic defects derived from the observed data divided by temperature, $n_i C_i/T$, vs. T for the $YBa_2Cu_3O_7$ pellet sample in a field of 70 kG (open circles). The solid curve is the theoretical prediction for n_i = 0.0044 moles of spin 1/2 defects per mole of $YBa_2Cu_3O_7$.

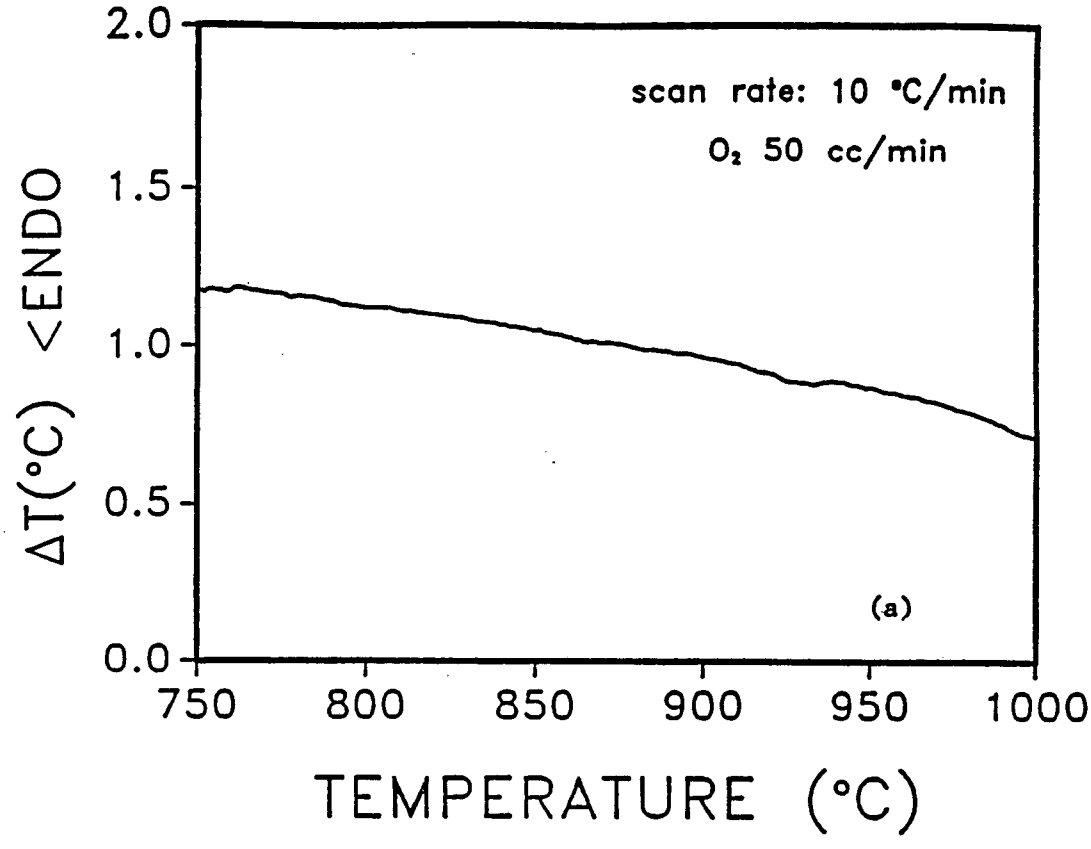
2.0
1.5
1.0
0.5
0.0
ΔT(°C) <ENDO
scan rate: 10 °C/min
O₂ 50 cc/min
(a)
750
800
850
900
950
1000
TEMPERATURE (°C)

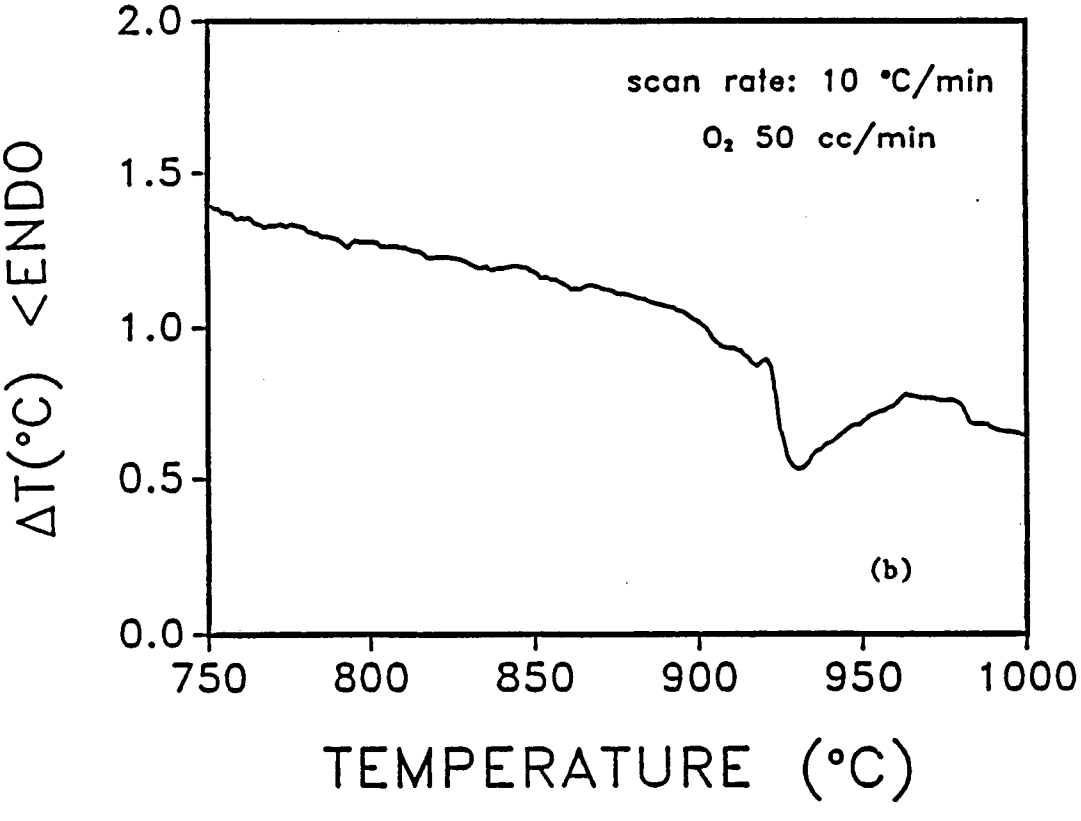
2.0
1.5
1.0
0.5
0.0
ΔT(°C) <ENDO
scan rate: 10 °C/min
O₂ 50 cc/min
(b)
750
800
850
900
950
1000
TEMPERATURE (°C)

Figure 1

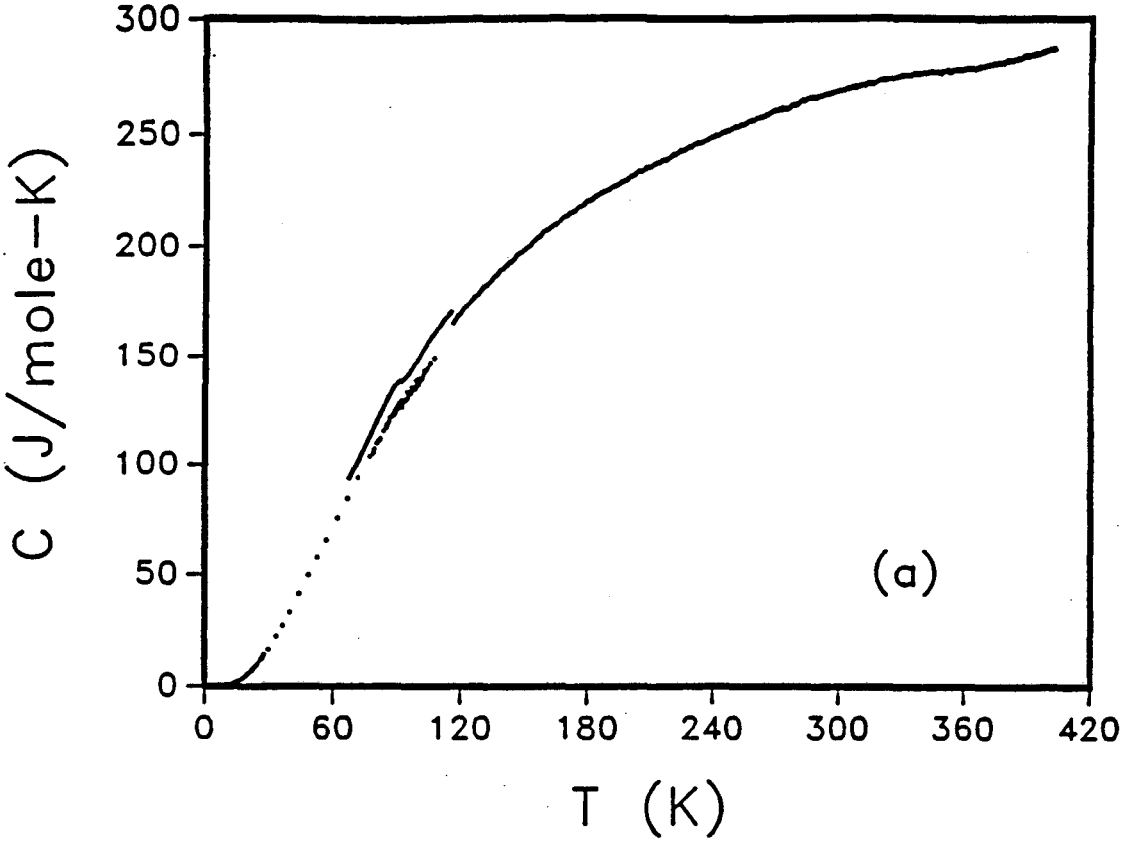
C (J/mole-K)
300
250
200
150
100
50
0
0
60
120
180
240
300
360
420
T (K)
(a)

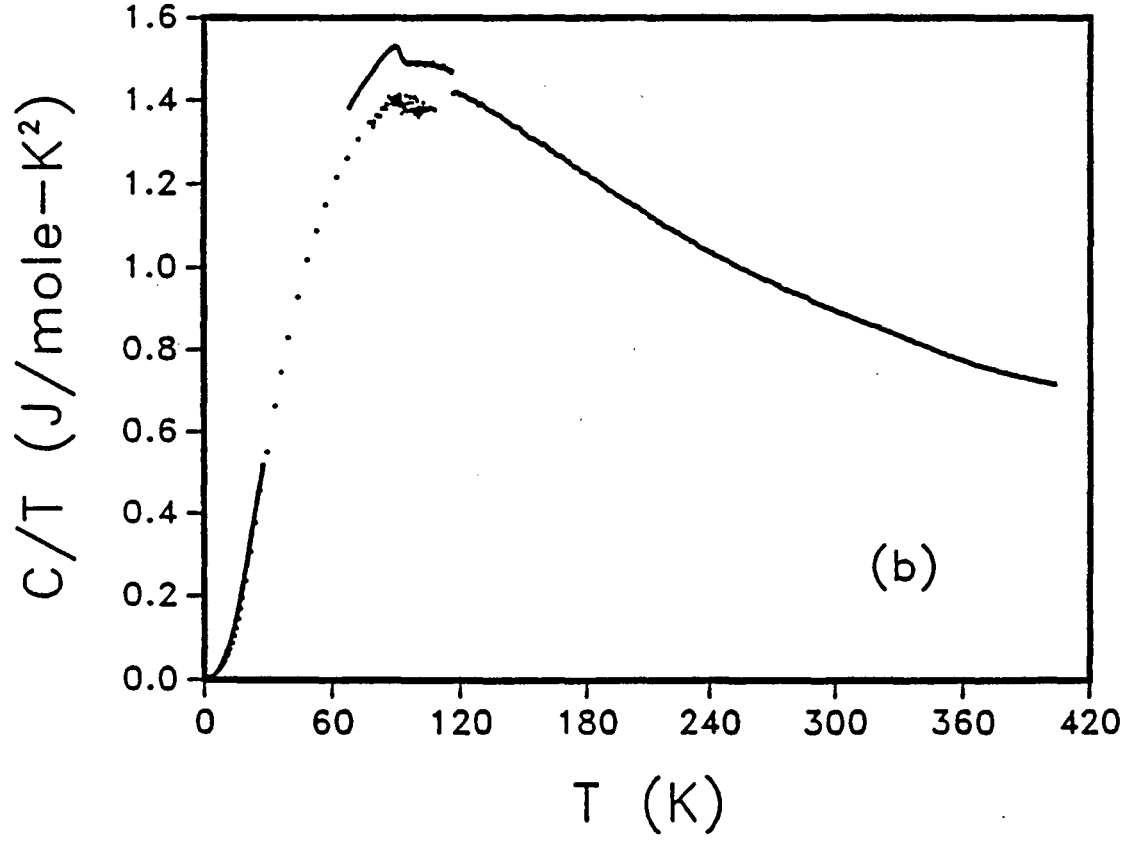
C/T (J/mole-K²)
1.6
1.4
1.2
1.0
0.8
0.6
0.4
0.2
0.0
0
60
120
180
240
300
360
420
T (K)
(b)

Figure 2

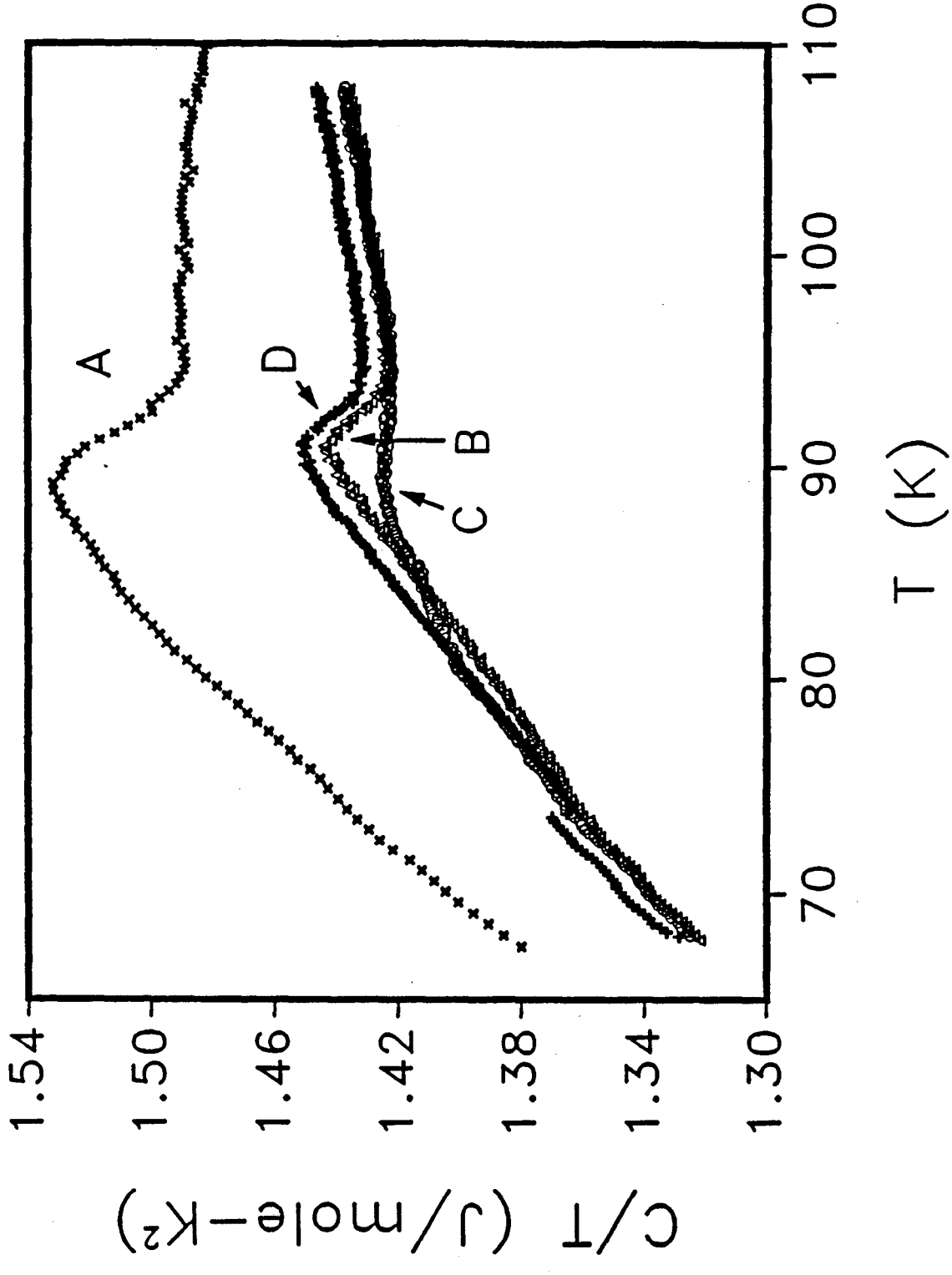

Figure 3

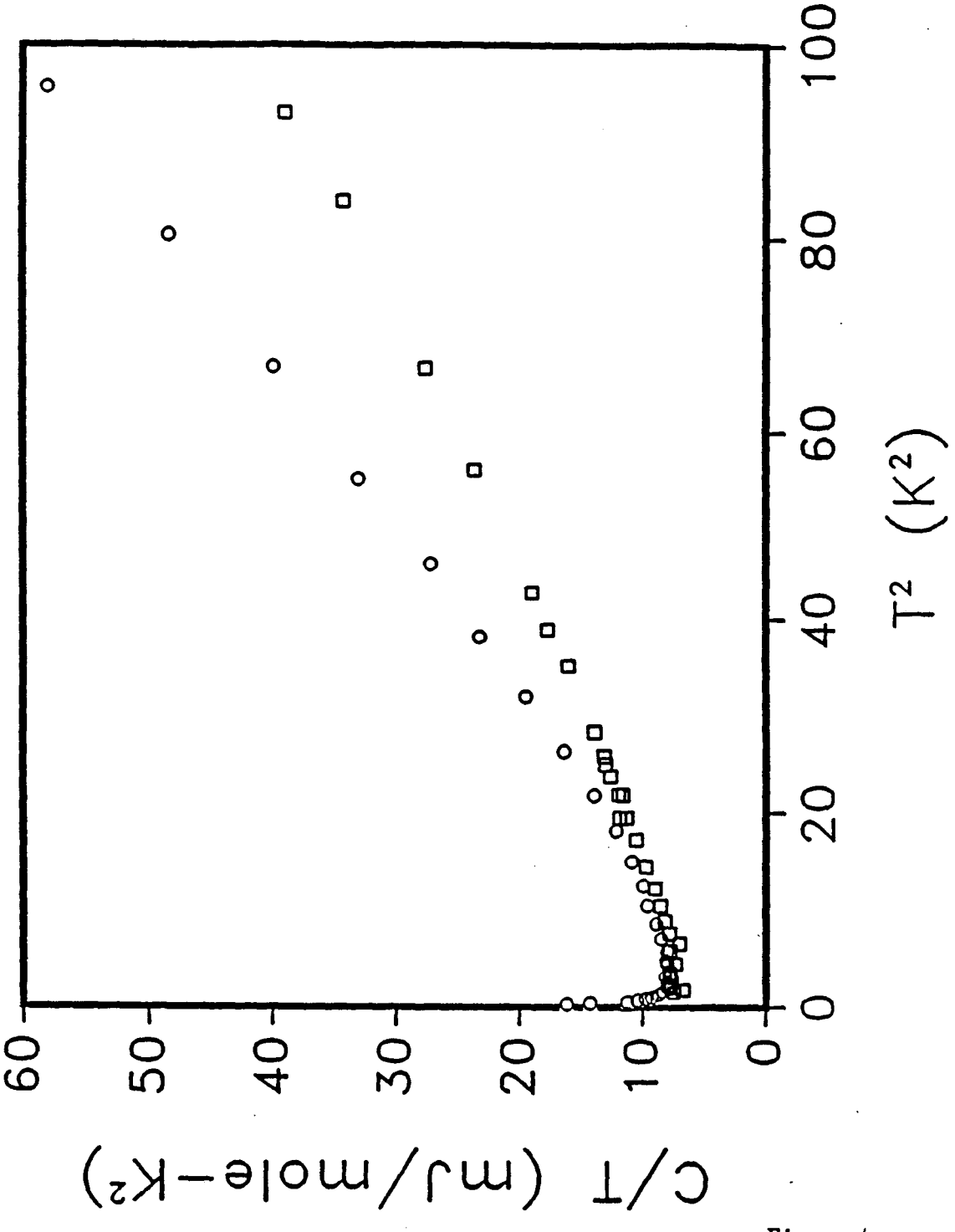

Figure 4

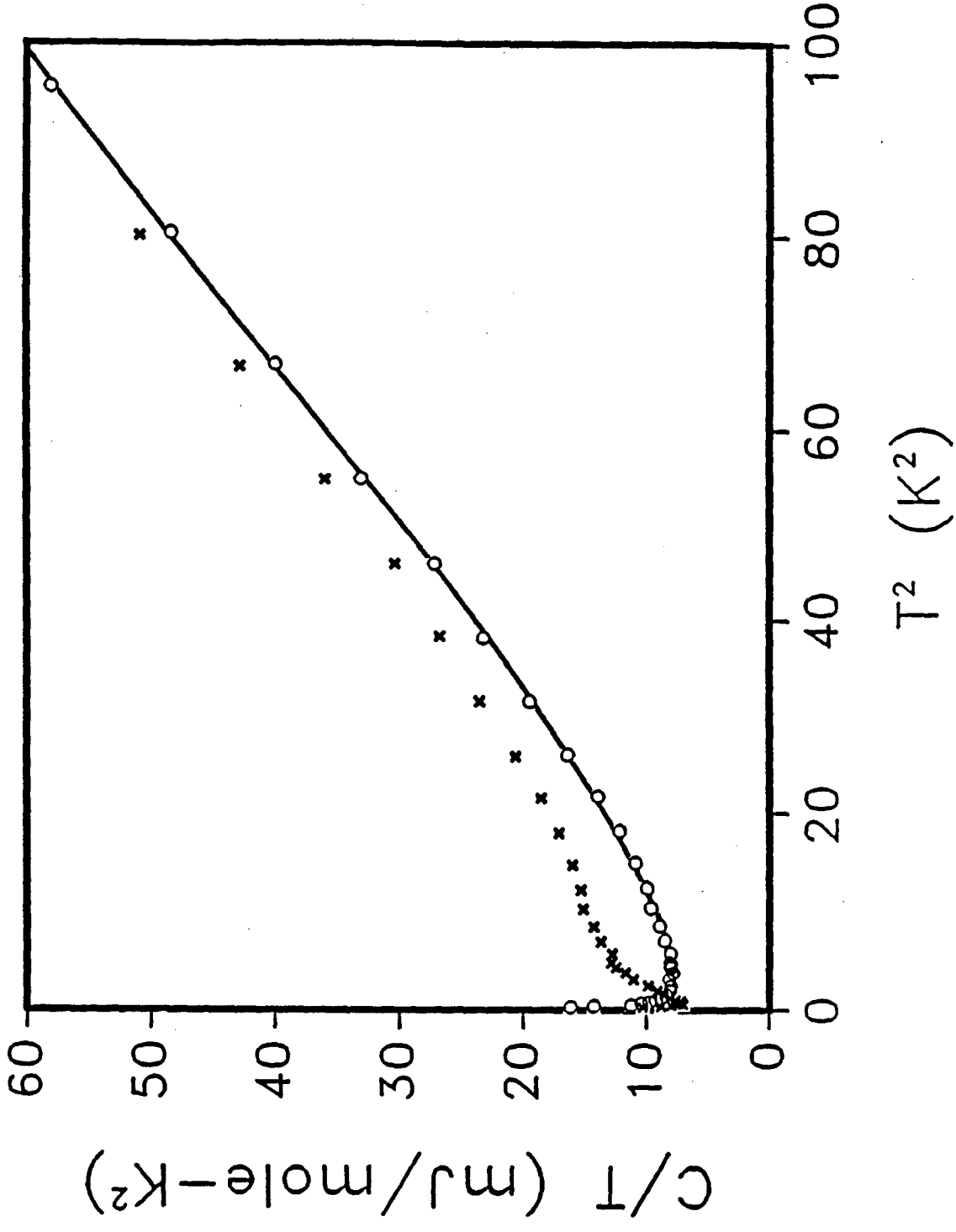

Figure 5

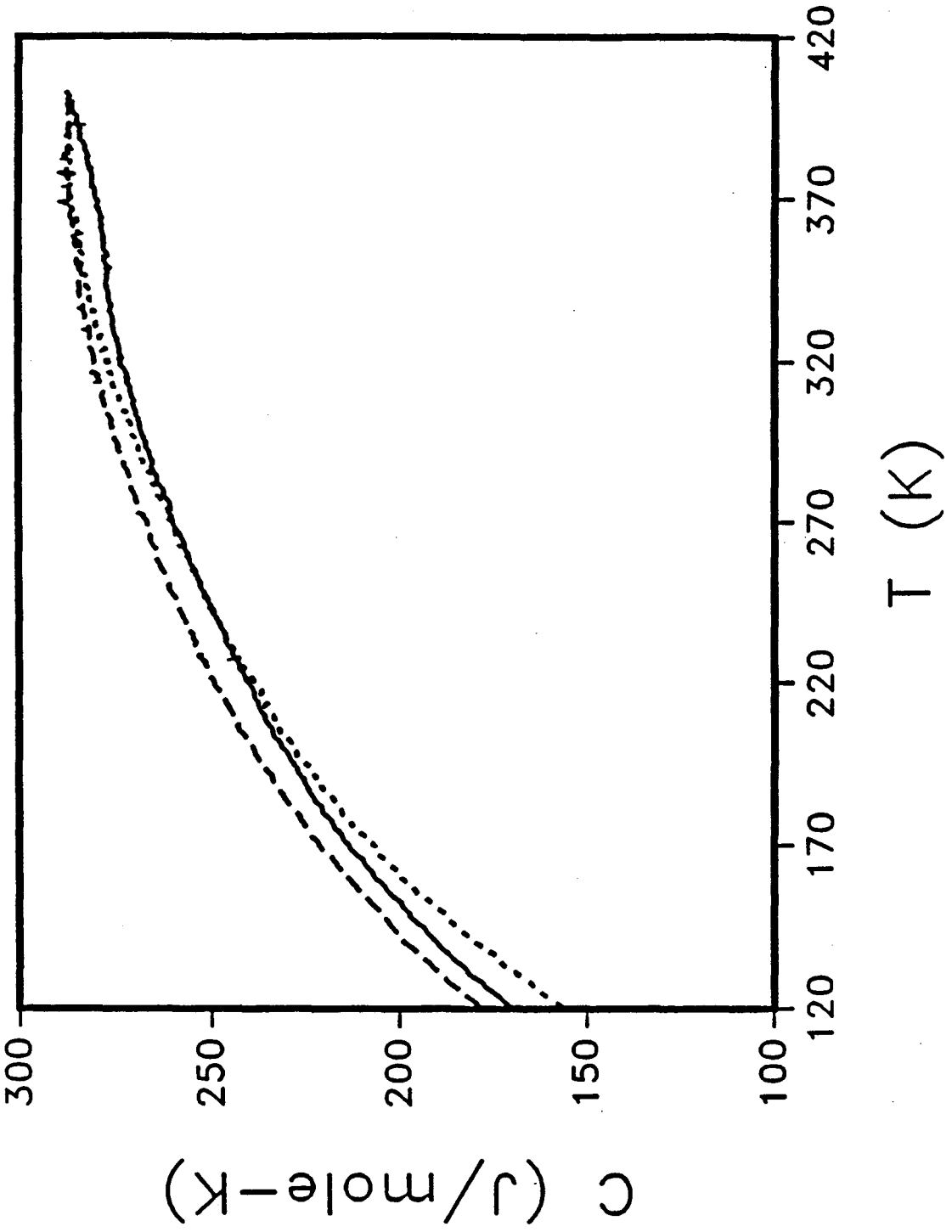

Figure 6

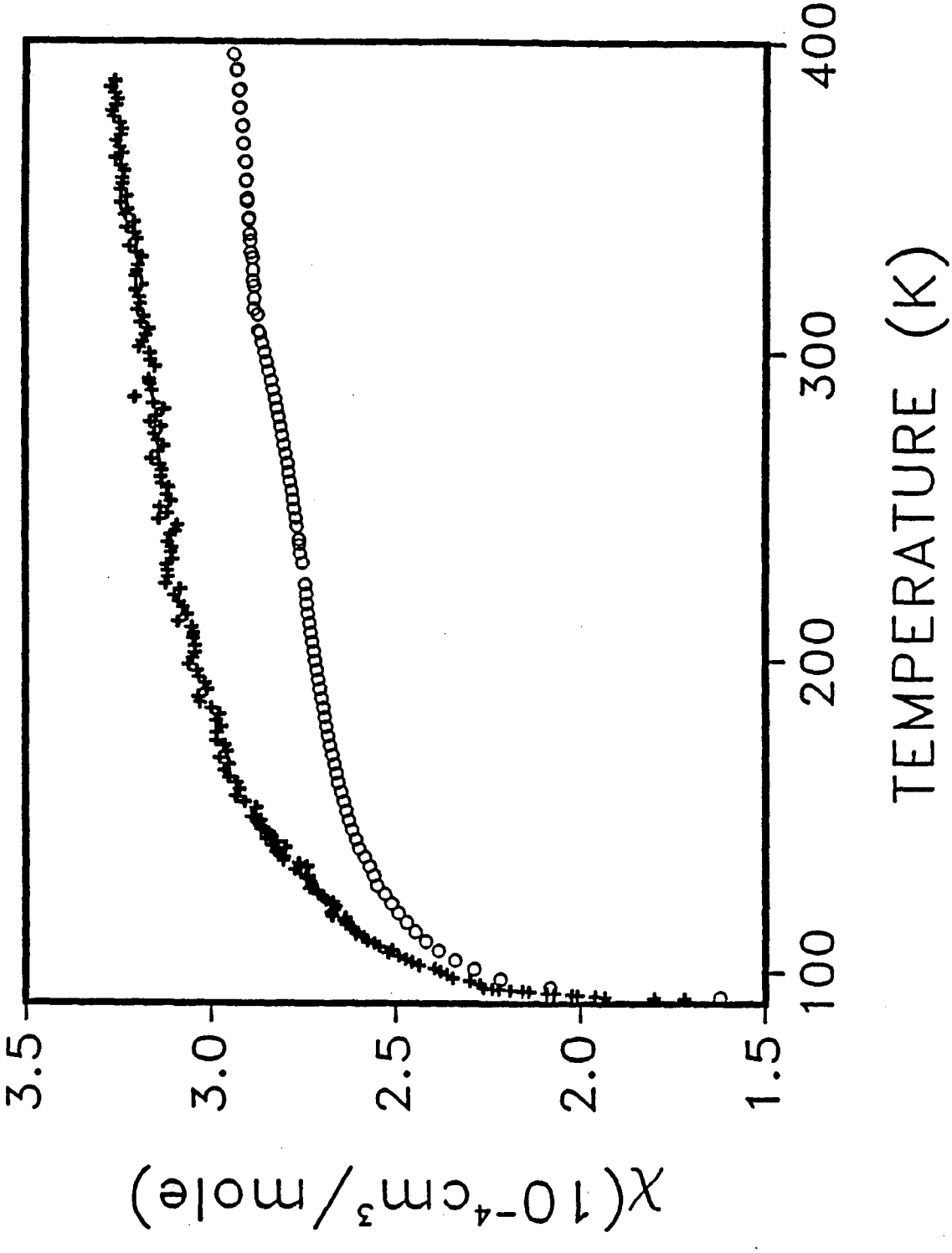

Figure 7

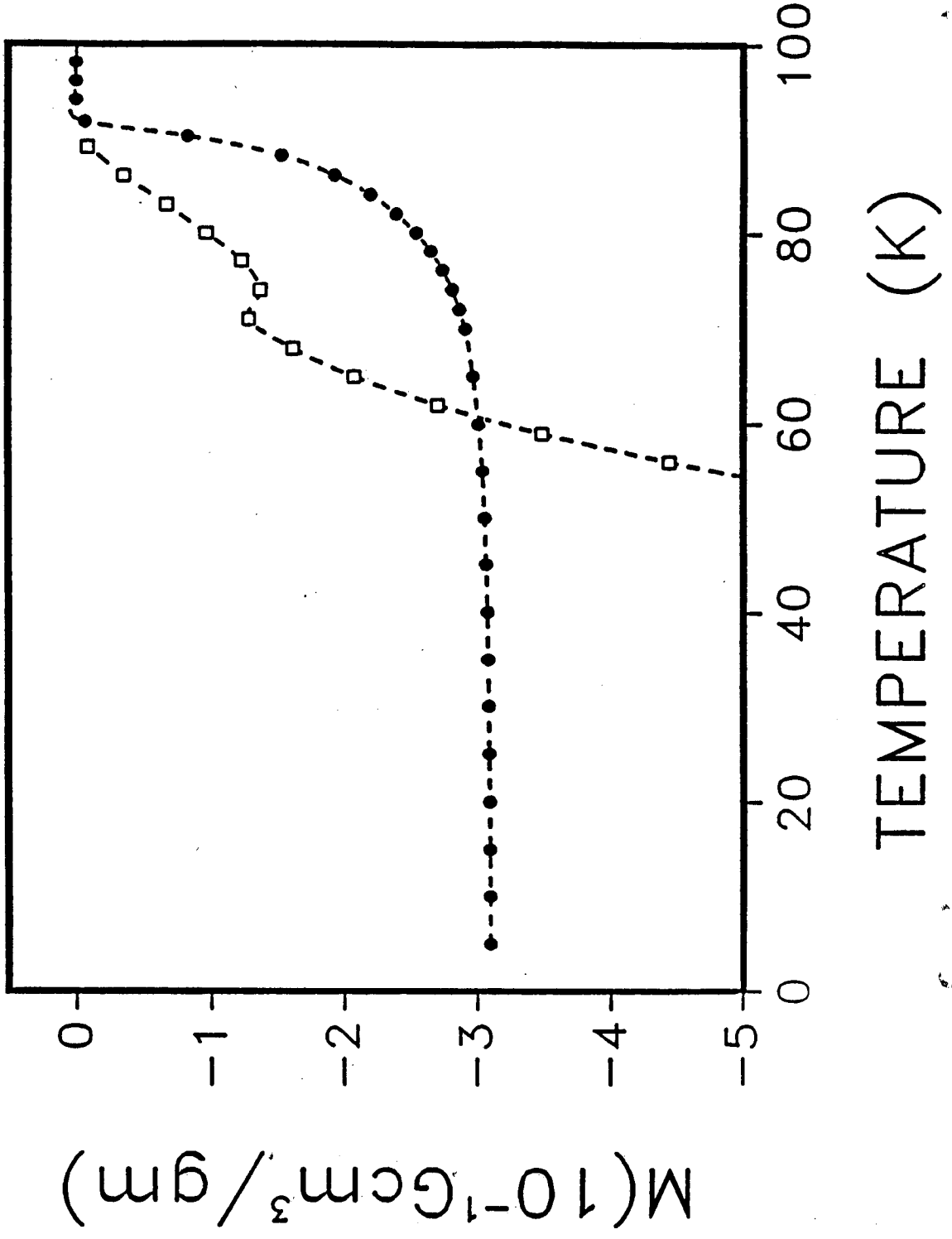

Figure 8

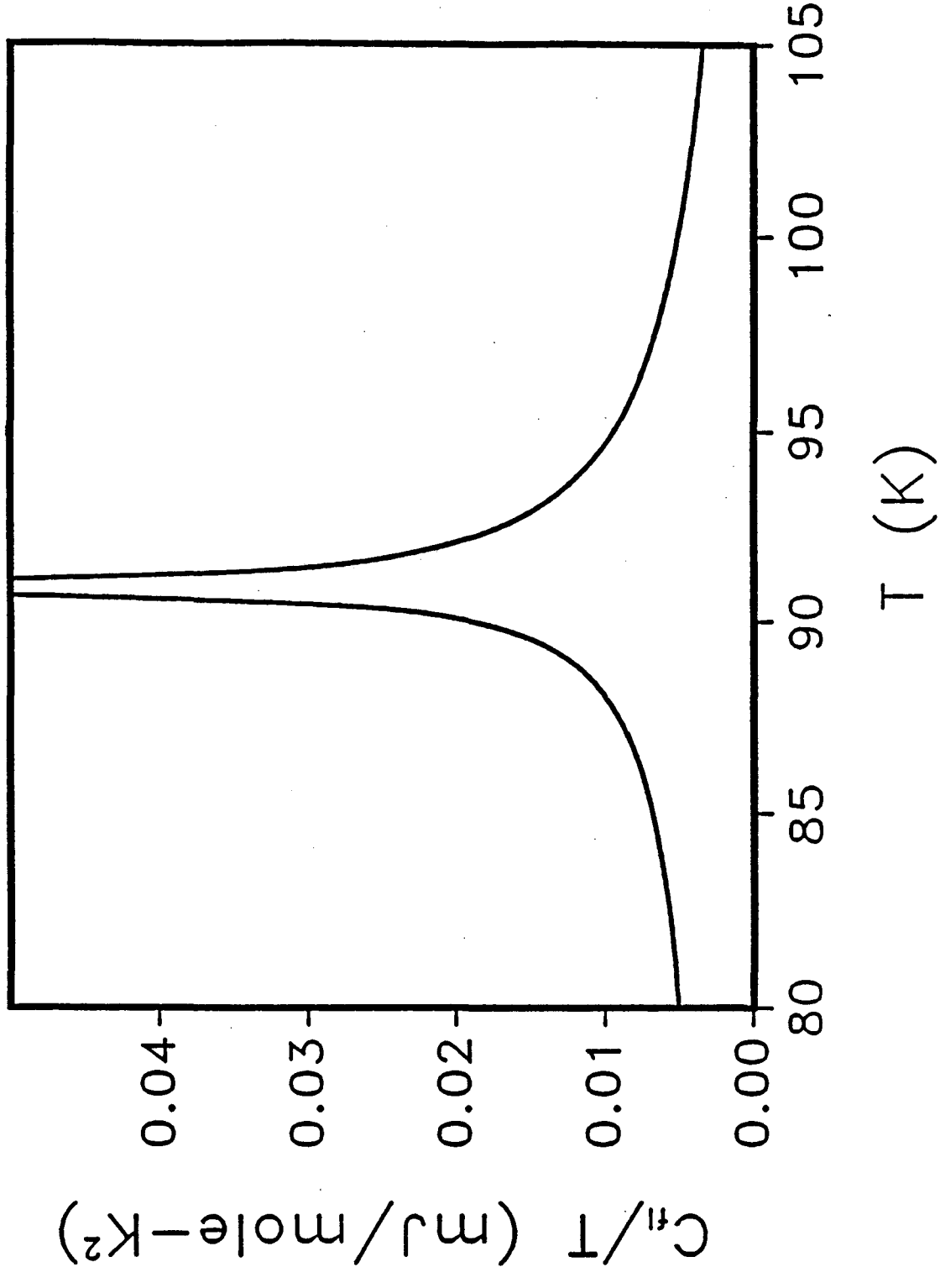

Figure 9

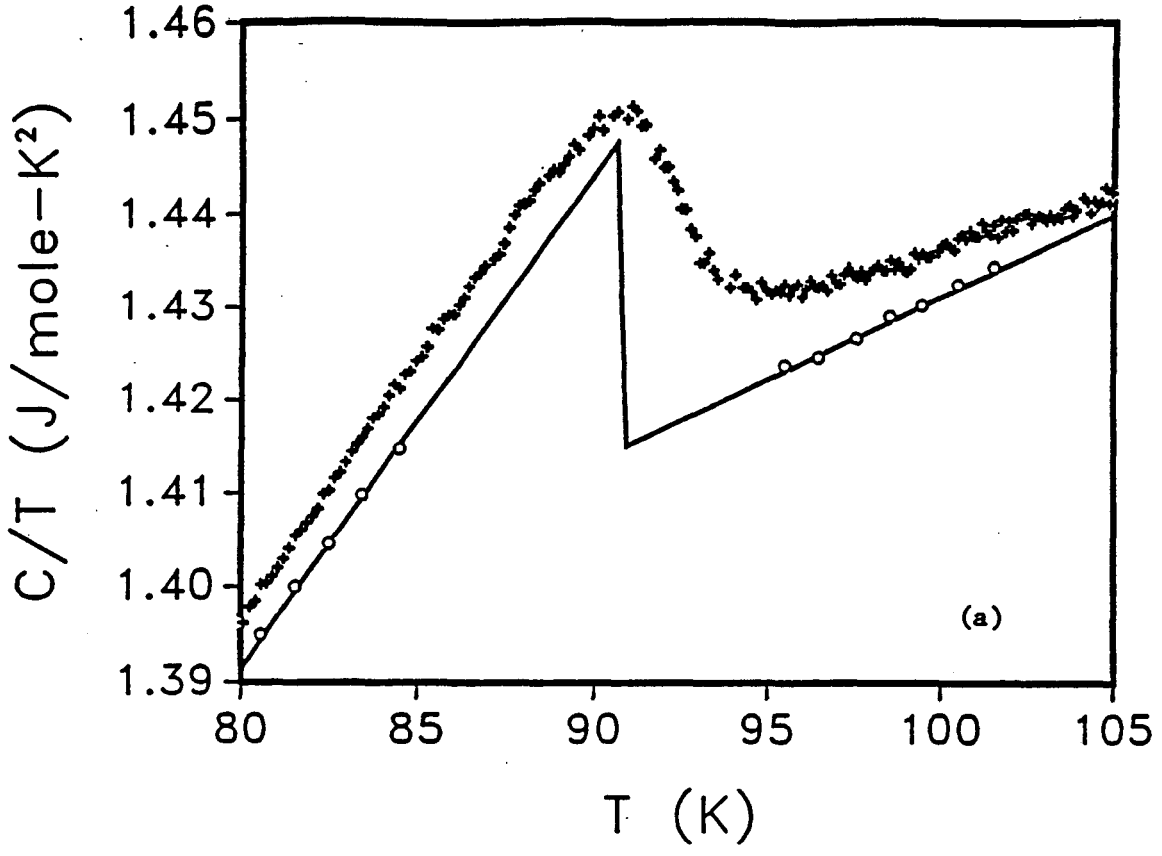
1.46
1.45
1.44
1.43
1.42
1.41
1.40
1.39
C/T (J/mole-K²)
(a)
80
85
90
95
100
105
T (K)

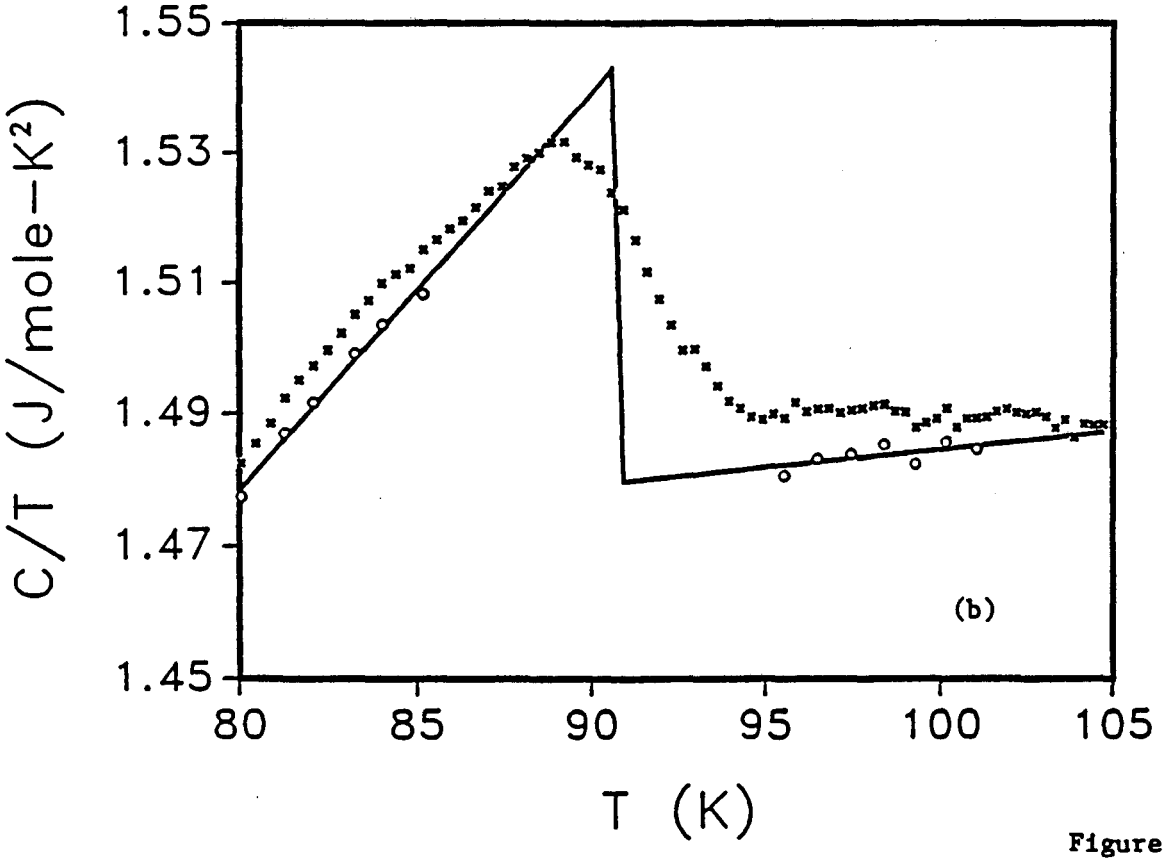
1.55
1.53
1.51
1.49
1.47
1.45
C/T (J/mole-K²)
(b)
80
85
90
95
100
105
T (K)

Figure 10

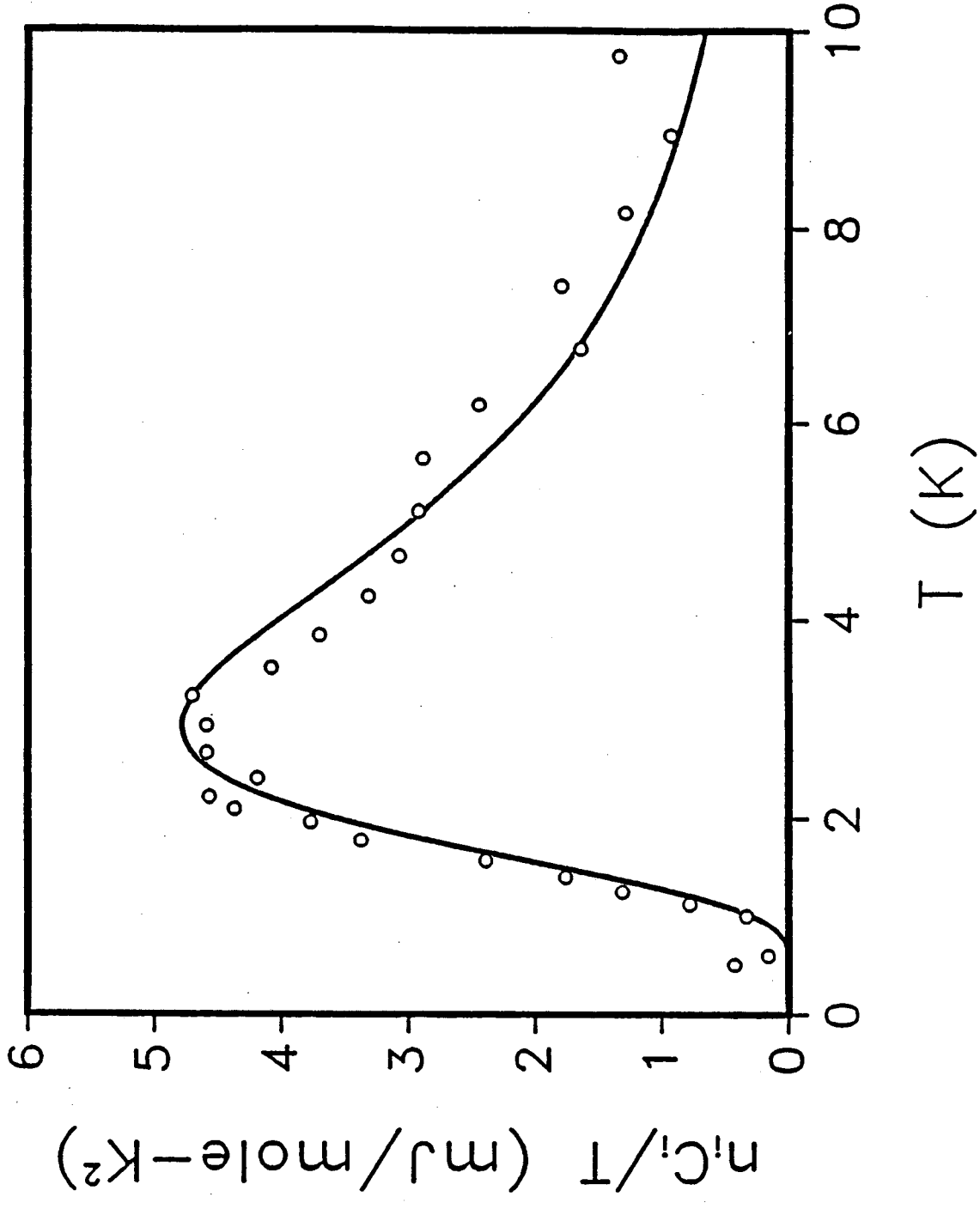

Figure 11

LAWRENCE BERKELEY LABORATORY
UNIVERSITY OF CALIFORNIA
INFORMATION RESOURCES DEPARTMENT
BERKELEY, CALIFORNIA 94720